

## **General Disclaimer**

### **One or more of the Following Statements may affect this Document**

- This document has been reproduced from the best copy furnished by the organizational source. It is being released in the interest of making available as much information as possible.
- This document may contain data, which exceeds the sheet parameters. It was furnished in this condition by the organizational source and is the best copy available.
- This document may contain tone-on-tone or color graphs, charts and/or pictures, which have been reproduced in black and white.
- This document is paginated as submitted by the original source.
- Portions of this document are not fully legible due to the historical nature of some of the material. However, it is the best reproduction available from the original submission.

# NASA TECHNICAL MEMORANDUM

NASA TM X- 73354

(NASA-TM-X-73354) LASER DOPPLER SYSTEMS IN  
ATMOSPHERIC TURBULENCE (NASA) 51 p HC  
A04/MF A01 CACL 20N

N77-14297

Unclas

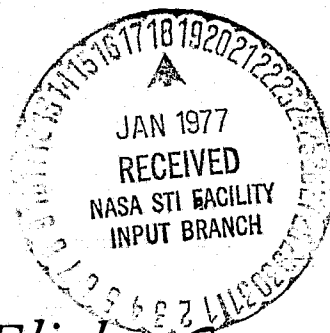
G3/32 59021

## LASER DOPPLER SYSTEMS IN ATMOSPHERIC TURBULENCE

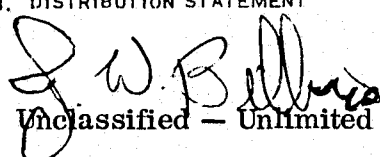
By S. S. R. Murty  
Electronics and Control Laboratory

November 1976

**NASA**



*George C. Marshall Space Flight Center  
Marshall Space Flight Center, Alabama*

1. REPORT NO. <b>NASA TM X-73354</b>		2. GOVERNMENT ACCESSION NO.		3. RECIPIENT'S CATALOG NO.	
4. TITLE AND SUBTITLE  <b>Laser Doppler Systems in Atmospheric Turbulence</b>				5. REPORT DATE <b>November 1976</b>	
				6. PERFORMING ORGANIZATION CODE	
7. AUTHOR(S) <b>S. S. R. Murty</b>				8. PERFORMING ORGANIZATION REPORT #	
9. PERFORMING ORGANIZATION NAME AND ADDRESS  <b>George C. Marshall Space Flight Center Marshall Space Flight Center, Alabama 35812</b>				10. WORK UNIT NO.	
				11. CONTRACT OR GRANT NO.	
12. SPONSORING AGENCY NAME AND ADDRESS  <b>National Aeronautics and Space Administration Washington, D.C. 20546</b>				13. TYPE OF REPORT & PERIOD COVERED  <b>Technical Memorandum</b>	
				14. SPONSORING AGENCY CODE	
15. SUPPLEMENTARY NOTES  <b>Prepared by Electronics and Control Laboratory, Science and Engineering</b>					
16. ABSTRACT  <p>This report is concerned with the estimation of the loss of heterodyne signal power for the Marshall Space Flight Center laser Doppler system due to the random changes in the atmospheric index of refraction. The current status in the physics of low-energy laser propagation through turbulent atmosphere is presented, as well as the analysis and approximate evaluation of the loss of the heterodyne signal power due to the atmospheric turbulence. The losses due to the atmospheric absorption, scattering, and turbulence are estimated for the conditions of the January 1973 flight tests, and theoretical and experimental signal to noise values are compared. In addition, the maximum and minimum values of the atmospheric attenuation over a two-way path of 20 km range are calculated as a function of altitude using models of atmosphere, aerosol concentration, and turbulence.</p>					
17. KEY WORDS			18. DISTRIBUTION STATEMENT   <b>Unclassified - Unlimited</b>		
19. SECURITY CLASSIF. (of this report)  <b>Unclassified</b>		20. SECURITY CLASSIF. (of this page)  <b>Unclassified</b>		22. PRICE  <b>NTIS</b>	
				21. NO. OF PAGES  <b>51</b>	

## ACKNOWLEDGMENTS

The author is very grateful to his Scientific Advisor, Mr. R. M. Huffaker, for introducing him to this fascinating subject, and to Mr. C. O. Jones who has provided immense support during the work covered in this report. The author has also benefited greatly from long discussions with Dr. L. Z. Kennedy and expresses his sincere appreciation. In addition the discussions with Dr. J. L. Randall, Mr. F. W. Wagnon, Mr. E. A. Weaver, Mr. J. A. Dunkin, Mr. J. W. Bilbro, Mr. R. W. George, and Mr. H. B. Jeffreys are gratefully acknowledged.

## TABLE OF CONTENTS

	Page
I. INTRODUCTION .....	1
II. PARAMETERS OF ATMOSPHERIC TURBULENCE .....	2
III. OPTICAL PROPERTIES OF THE TURBULENT EDDIES .....	4
IV. EFFECT OF ATMOSPHERIC TURBULENCE ON LASER BEAMS .....	9
V. EFFECT OF TURBULENCE ON HETERODYNE LASER DOPPLER SYSTEMS .....	23
VI. CALCULATION OF S/N LOSS FOR THE MSFC SYSTEM ...	24
VII. CONCLUSIONS .....	39
REFERENCES .....	41

## LIST OF ILLUSTRATIONS

	Page
1. Three-dimensional turbulence spectrum models for index-of-refraction fluctuation . . . . .	5
2. Saturation of the variance of log-amplitude fluctuations of a spherical wave propagating through a homogeneous ( $C_n^2 = \text{const.}$ ) turbulence path . . . . .	16
3. Theoretical curves of the log-amplitude covariance function in weak to strong turbulence . . . . .	19
4. Block diagram of the MSFC pulsed laser Doppler system . . .	25
5. Comparison of measured and theoretical S/N values . . . . .	36
6. Atmospheric attenuation at $10.6 \mu\text{m}$ . . . . .	38

## LIST OF TABLES

	Page
1. Comparison of Losses at $\text{CO}_2$ and DF Laser Wavelengths Over a 20 km Horizontal Path at 2.5 km and 5 km Altitudes . . . . .	37
2. Signal Loss in Atmospheric Propagation at $10.6 \mu\text{m}$ Due to Absorption, Scattering and Coherence Degradation for a Two-Way Horizontal Path of 20 km at Each Altitude . . . . .	39

## LASER DOPPLER SYSTEMS IN ATMOSPHERIC TURBULENCE

### I. INTRODUCTION

Marshall Space Flight Center (MSFC) has been developing laser Doppler systems, pulsed and continuous wave, for remote measurement of wind speed and turbulence for over a decade. A discussion of these systems is given by Huffaker [1-4]. The pulsed system, designed to operate over long atmospheric paths, is affected by attenuation due to atmospheric gases, particulate matter, and turbulence. The transmission loss experienced by the pulsed system has been worked out in detail in Reference 5. The effects of atmospheric turbulence on the performance of the laser Doppler system are considered in this report. A discussion of the basic effects experienced by a laser beam propagating in the normal atmosphere is presented first.

The atmospheric turbulence manifested in random temperature fluctuations causes optical effects long known to astronomers as twinkling (variation of image brightness), quivering (displacement of image from normal position), tremor disk (smearing of the diffraction image), dancing (continuous movement of a star image about a mean point), wandering (slow oscillatory motions of the image with a period of approximately 1 min and angular excursions of a few seconds of arc), pulsation or breathing (fairly rapid change of size of the image), image distortion, and boiling (time-varying nonuniform illumination in a larger spot image) [6]. In the case of a laser beam, the turbulence effects are broadly categorized as beam wander, spot dancing, beam spread, and scintillations. These effects are observed due to the temporal and spatial fluctuations of the direction, phase, and intensity of the wavefront. A description of the atmospheric inhomogeneities causing the effects mentioned is given in the next section.

## II. PARAMETERS OF ATMOSPHERIC TURBULENCE

The optical effects of interest are produced by the variations of refractive index along the path of the beam. The changes in the refractive index are caused by the fluctuations of temperature which arise in turbulent mixing of various thermal layers. It is found that the temperature fluctuations obey the same spectral law as the velocity fluctuations. In analogy with the velocity turbulence, the atmosphere may be imagined to consist of a large number of eddies with varying dimensions and refractive indices. For isotropic turbulence, the velocity spectrum  $\phi_v(K)$  (where the wavenumber  $K = 2\pi/\ell$ ,  $\ell$  being the size of a turbulent eddy) contains the information about the turbulence.  $\phi_v(K)$  is intuitively interpreted as the amount of energy in the turbulent eddies of size  $\ell$ . The kinetic energy of turbulence is assumed to be introduced through eddy scale sizes larger than the "outer scale" of turbulence,  $L_0$ , corresponding to a spatial wavenumber  $K_0 = 2\pi/L_0$ . As the wavenumber increases beyond  $K_0$ , the turbulence tends to become isotropic and homogeneous. Experiments have confirmed the predictions of Kolmogorov's theory of  $K^{-11/3}$  dependence for the three-dimensional spectrum up to wavenumber  $K_m$  related to the inner scale of turbulence  $\ell_0$  by  $K_m = 5.92/\ell_0$ . The spectrum in the dissipation region for which the scale sizes are smaller than  $\ell_0$  or wavenumbers greater than  $K_m$  is steeper than  $K^{-11/3}$ . The spatial wavenumber region between the inner scale  $\ell_0$  and the outer scale  $L_0$  obeying the Kolmogorov theory of a spectral slope of  $-11/3$  is known as the inertial subrange.  $\ell_0$  is of the order of several millimeters and  $L_0$  several meters.

At optical wavelengths the refractive index may be related to the temperature through the relation

$$n_1 = n - 1 = \frac{77.6 P}{T} \left[ 1 + \frac{0.00753}{\lambda^2} \right] \times 10^{-6} \quad (1)$$

where  $n$  is the refractive index,  $P$  is pressure in mb,  $T$  is temperature in K, and  $\lambda$  is wavelength in  $\mu\text{m}$ . The refractive index structure constant  $C_n^2$  is a measure of the strength of atmospheric turbulence and is defined as the



mean-square difference in the refractive index at two points divided by the separation distance  $r$  raised to the  $2/3$  power, i. e. ,

$$C_n^2 = \frac{\langle (n_2 - n_1)^2 \rangle}{r^{2/3}} \quad . \quad (2)$$

The temperature structure constant  $C_T^2$  is similarly defined for temperature fluctuations. Thus  $C_n$  may be determined from temperature measurements alone from the following relation:

$$C_n = \frac{77.6 P}{T^2} \left[ 1 + \frac{0.00753}{\lambda^2} \right] \times 10^{-6} C_T \quad . \quad (3)$$

Typical temperature variations of approximately 1 K resulting in refractive index variations of a few parts in a million will cause significant effects on optical radiation fields propagating through the atmosphere.  $C_n^2$  is measured in units of (meters)<sup>-2/3</sup> and varies from  $10^{-13}$  or more for strong turbulence to  $10^{-17}$  or less for weak turbulence.

Assuming that the form of the temperature spectrum and the refractive index spectrum is the same as that of the velocity spectrum, Tatarski [7] gave the following form for the refractive index spectrum:

$$\phi_n(K) = 0.033 C_n^2 K^{-11/3} \exp\left(\frac{-K^2}{K_m^2}\right) \quad (4)$$

where  $K_m = 5.92$ . This spectrum has a singularity at  $K = 0$ . Physically the singularity implies that the energy per unit volume becomes unbounded as the eddy size increases. This singularity is avoided by using the modified von Karman spectrum [8]:

$$\phi_n(K) = \frac{0.033 C_n^2 \exp \left[ -K^2 \left( \frac{\ell_0}{2\pi} \right)^2 \right]}{\left[ K^2 + \left( \frac{L_0}{2\pi} \right)^2 \right]^{11/6}} \quad (5)$$

which gives a bounded variation for  $K < 2\pi/L_0$ . The three dimensional refractive index spectrum models according to equations (4) and (5) are shown in Figure 1. Deviations from these models occur if the turbulence is not homogeneous. Deviations have been observed in measurements over paths close to the ground and under conditions of weak turbulence [8]. The optical effects of the eddies are considered in the next section.

### III. OPTICAL PROPERTIES OF THE TURBULENT EDDIES

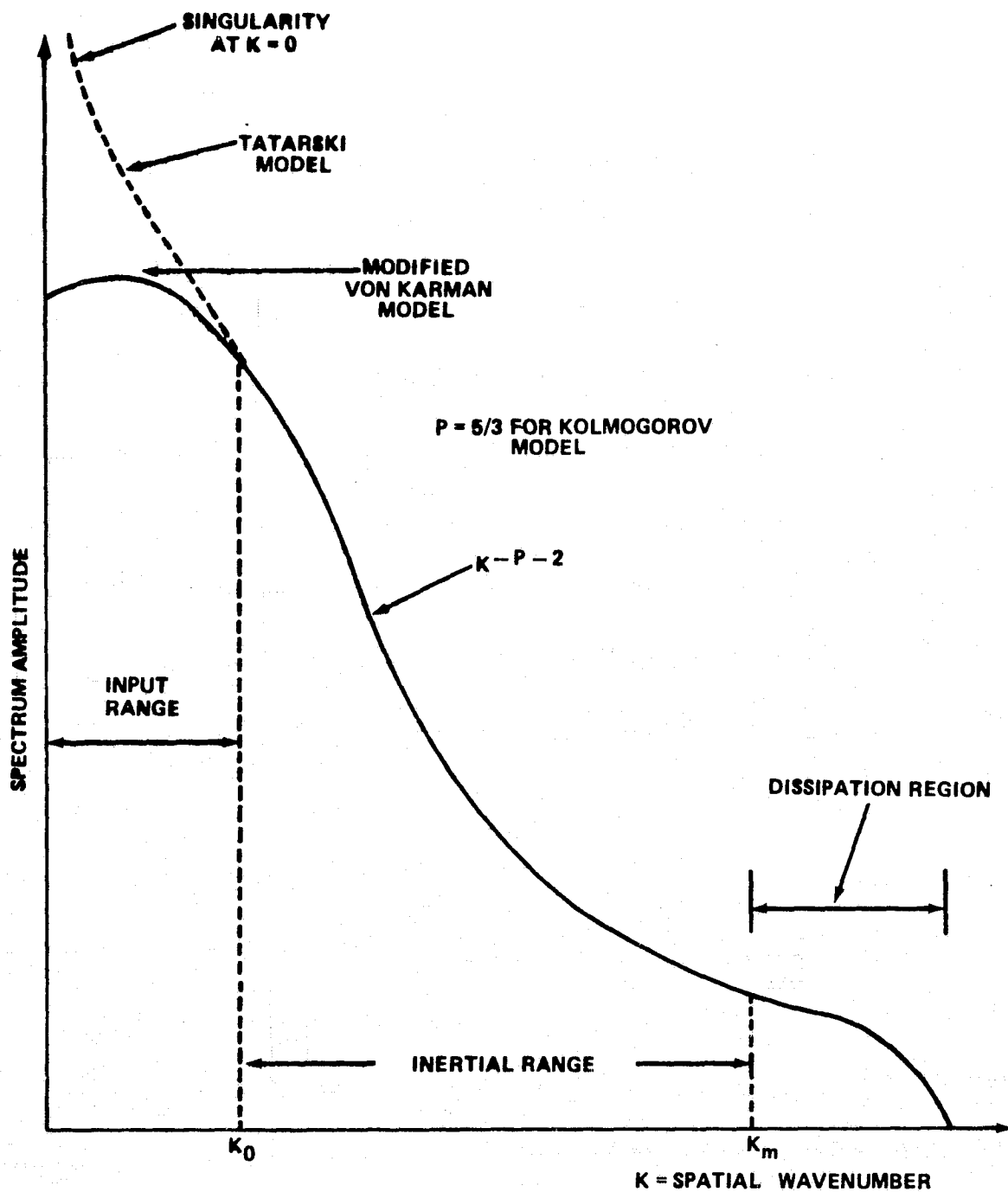
The optics of the turbulent atmosphere may be described in terms of a collection of weak, moving, three-dimensional, gaseous lenses of varying scale sizes bounded by the inner scale  $\ell_0$  and the outer scale  $L_0$  of the turbulence. From equation (2), it may be seen that the refractive index fluctuations associated with any scale size  $\ell$  increases as the size of the eddy increases:

$$\langle [\delta n(\ell)]^2 \rangle = C_n^2 \ell^{2/3} \quad (6)$$

An eddy of radius  $\ell$  can act as a lens with a focal length  $f = R/n_1$ , where  $R$  is the radius of lens curvature. This is approximated as

$$f \sim \frac{\ell}{n_1} \approx \ell^{2/3} C_n^{-1}$$

from equation (6). Turbulence as it naturally occurs can consist of eddies of hot and cold air. Eddies cooler than the ambient air have a higher index of refraction. In this case,  $n_1$  is positive and the lens is convergent. If the eddy



$K = 2\pi/\ell$  WHERE  $\ell$  = SIZE OF TURBULENCE EDDY;  
 $K_0 = 2\pi/L_0$ , TYPICALLY  $L_0 = 1 - 100$  m;  
 $K_m = 2\pi/\ell_0$ , TYPICALLY  $\ell_0 = 1 - 3$  mm

Figure 1. Three-dimensional turbulence spectrum models for index-of-refraction fluctuation.

consists of warmer air, the index of refraction is lower (giving negative  $n_1$ ) and the lens is divergent. Typical values in the atmosphere are  $C_n \sim 10^{-7}$ ,  $|n_1| \sim 10^{-6}$ , and  $\ell$  a few centimeters. Thus the focal length of the atmospheric lenses is  $f \sim 10$  km.

The turbulent eddies cause diffraction and refraction of the optical wavefront, and it is instructive to consider these two effects separately. Each eddy of size  $\ell$  bends a ray bundle individually and has a diffraction pattern of approximate width,  $\lambda L / \ell$ , where  $L$  is the distance from the eddy to the receiver. The diffraction effects are negligible if  $\lambda L / \ell \ll \ell$  or if  $\ell \gg \sqrt{\lambda L}$ , and this is the geometric optics regime. But if  $\lambda L / \ell \gg \ell$  the diffraction pattern entirely determines the intensity distribution of the receiver. Thus the distance  $L_d$  beyond which the diffraction effects are important may be defined by  $L_d \sim \ell^2 / \lambda$ .

The refractive bending of rays by an eddy of size  $\ell$  depends on the refractive index of the eddy and may be calculated by Snell's law to give  $\delta\theta \sim \delta n$ .  $\delta n$  is zero on the average. The mean square angular fluctuation for one eddy is  $\langle (\delta\theta)^2 \rangle \sim \langle (\delta n)^2 \rangle$ .

Over a path length  $L$ , let the beam traverse  $L/\ell$  eddies. Since the deflections are uncorrelated from one eddy to another, they add up as mean squares and the total mean square deflection is

$$\langle \theta_r^2 \rangle \sim \frac{L}{\ell} \langle (\delta n)^2 \rangle = C_n^2 L \ell^{-1/3} \quad (7)$$

The effect of refraction is to change the cross section of the beam from  $\ell^2$  to  $(\ell \pm L\theta_r)^2$ . The amplitudes of the wave before and after refraction are related as

$$A^2 \ell^2 = (A + \Delta A)^2 (\ell \pm L\theta_r)^2$$

The fractional amplitude change is then given by

$$X = \frac{\Delta A}{A} \sim \frac{L}{\ell} \theta_r$$

The variance of the amplitude fluctuation is then given by

$$\langle X^2 \rangle \sim \frac{L^2}{\ell^2} \langle \theta_r^2 \rangle \sim C_n^2 L^3 \ell^{-7/3} . \quad (8)$$

The particular scale size 1 which contributes predominantly to the amplitude fluctuation depends on the path length; i.e., different eddies are more effective at different path lengths in producing amplitude fluctuations. This point has been discussed by Tatarski [9] and De Wolf [10] as follows.

There are no diffraction effects in equation (8). Diffraction effects are negligible if the path length  $L_s$  is short or  $L_s \ll \ell_0^2/\lambda$  in the geometric optics regime. Since  $\ell_0$  (inner scale length) is the smallest eddy size, the diffraction by eddies of all sizes is negligible in this case. The smallest eddies then have the largest contribution. Equation (8), then becomes

$$\langle X^2 \rangle \sim C_n^2 L_s^3 \ell_0^{-7/3} \quad \text{for} \quad L_s \ll \frac{\ell_0^2}{\lambda} . \quad (9)$$

For path lengths  $L_\ell$  greater than  $L_s$ , such that  $L_\ell \gg \ell_0^2/\lambda$ , the eddies with sizes greater than  $\ell_\ell$  ( $\ell > \ell_\ell$ ) have negligible diffraction, while eddies with sizes smaller than  $\ell_\ell$  ( $\ell < \ell_\ell$ ) diffract the rays where

$$\ell_\ell = \sqrt{\lambda L_\ell} .$$

The diffraction pattern entirely determines the intensity distribution and the refraction is negligible for the small eddies of size  $\ell \ll \ell_\ell$ ; i.e., these eddies simply scatter the energy, not focusing the rays, and have little effect on the amplitude fluctuations. Geometric optics results may still be applied if the eddies of size  $\ell < \ell_\ell$  are excluded. Then the smallest eddy size contributing significantly to the amplitude fluctuation is  $\ell_\ell$  and  $\ell = \ell_\ell$  is substituted in equation (8):

$$\langle X^2 \rangle \sim C_n^2 L_\ell^3 (\lambda L_\ell)^{-7/6} \sim C_n^2 K^{7/6} L_\ell^{11/6} \quad \text{for } L_\ell \gg \frac{\ell_0^2}{\lambda} \quad (10)$$

This is also the result obtained by the Rytov approximation. Equation (10) has been interpreted by Tatarski [9] as the result of the application of geometrical optics to a medium from which all eddies of scale sizes less than  $\sqrt{\lambda L}$  have been removed.

A qualitative description of the effect of the optical inhomogeneities on the wavefront is sometimes helpful and is presented here. As a plane wavefront passes through a region of relatively lower refractive index, the wavefront will advance as the speed of light is higher. When passing through a region of higher refractive index, the wavefront is slowed down. Thus the refractive inhomogeneities of the atmosphere deform the wavefronts. Portions of the wavefront may be convex or concave in the direction of propagation. The concave portions converge while the convex portions diverge. Thus it is possible for the intensity to build up in some areas. Since the inhomogeneities are random and moving, the bright and the dark areas move randomly. This point of view has been developed by the optical astronomers [6].

Young [11] obtained equation (10) on considering an aperture of Fresnel-zone size while calculating the normalized variance or the total modulation power obtained with a circular aperture using geometric optics. He observed that ray optics gave the correct parametric dependence because very little power is contributed by the range of spatial frequencies greater than  $(\lambda L)^{-1/2}$  which are in the wave optics regime. Thus weak scintillation may be thought of as aperture filtering with a Fresnel-zone size aperture which filters out spatial frequencies higher than  $(\lambda L)^{-1/2}$ .

A related view developed by the radio astronomers is the phase screen concept. Immediately after passing through a layer of inhomogeneities, only the phase is affected and the intensity remains constant. As the distorted wavefront propagates further, the relative phases will be changed due to different directions of propagation and in this way, the amplitude fluctuations develop. This concept has been applied by Lee and Harp [12] to wave propagation by dividing the three-dimensional refractive field of the medium into thin slabs perpendicular to the direction of propagation. The effects of the refractive inhomogeneities on the propagation of laser beams in the atmosphere is discussed in the following section.

## IV. EFFECT OF ATMOSPHERIC TURBULENCE ON LASER BEAMS

A qualitative description of the effects based on the relative sizes of the beam and the refractive inhomogeneity is given first, followed by the results of Rytov approximation on the wave equation.

If the scale size of the inhomogeneity is much larger than the diameter of the laser beam, the entire beam is bent away from the line of sight and results in beam wander or beam steering. The center of the beam executes a two-dimensional random walk in the receiver plane and, for isotropic turbulence, the displacement of the beam from the line of sight will be Raleigh-distributed [13]. Inhomogeneities of the size of the beam diameter act as weak lenses on the whole or parts of the beam with a small amount of steering and spreading. When the inhomogeneities are much smaller than the beam diameter, small portions of the beam are independently diffracted and refracted and the phase front becomes corrugated. The propagation of the distorted phase front causes constructive interference over some parts of the receiver and destructive interference over others, leading to alternate bright and dark areas. Since the atmosphere is seldom stationary, the locations of the bright and dark regions change continually and give the pattern of "boiling." Thus, the turbulence causes the received field to scintillate in time and space. Since the atmosphere consists of inhomogeneities of all sizes in motion, the laser beam experiences fluctuations of beam size (spreading), beam position (steering or wander), and intensity distribution within the beam (scintillation) simultaneously. The relative importance of these effects depends on the path length, strength of turbulence, and the wavelength of the laser radiation. The variance of irradiance reflects the deviations from the mean due to beam wander, broadening, and scintillations. Estimates of these effects for finite beams are discussed as follows.

Finite transmitter effects have been treated by the Huygens-Fresnel approach [14] and by the transport approximation, Fante [15]. The Huygens-Fresnel principle was extended by Lutomirski and Yura [14] so that the secondary wavefront is determined by the envelope of spherical wavelets from the primary wavefront as in vacuum, but each wavelet is determined by the propagation of a spherical wave in the refractive medium for small scattering angles. Hence a knowledge of the spherical wave propagation in the turbulent medium is sufficient to determine the field distribution at an observation point. The mean irradiance distribution at the observation point is characterized by the

mutual coherence function (MCF) of a spherical wave and the geometry of the transmitting aperture. The MCF, defined as the cross-correlation function of the complex fields in a direction transverse to the direction of propagation, describes the loss of coherence of an initially coherent wave propagating in a random medium. When the medium is characterized by a refractive index variation that is gaussian with zero mean, the MCF is given by [7]

$$M(\rho, L) = \exp \left[ -\frac{1}{2} D(\rho) \right] \quad (11)$$

where  $D$  is the wave structure function,  $\rho$  is the lateral separation between the two points in a plane perpendicular to the direction of propagation, and  $L$  is the path length of propagation. For spherical wave propagation and a Kolmogorov spectrum of turbulence [16], the wave structure function is given by

$$D(\rho) = 2.91 K^2 \rho^{5/3} \int_0^L ds C_n^2(s) \left( \frac{s}{L} \right)^{5/3} . \quad (12)$$

For constant  $C_n^2$ ,

$$D(\rho) = 1.089 K^2 C_n^2 L \rho^{5/3} . \quad (13)$$

Equation (11) may be written as

$$M(\rho, L) = \exp \left[ -\left( \frac{\rho}{\rho_0} \right)^{5/3} \right] , \quad \ell_0 \ll \rho \ll L_0 , \quad (14)$$

where

$$\rho_0 = \left[ 1.455 K^2 \int_0^L ds C_n^2(s) \left( \frac{s}{L} \right)^{5/3} \right]^{-3/5} .$$



For constant  $C_n^2$

$$\rho_0 = [0.545 K^2 L C_n^2]^{-3/5} \quad (15)$$

$\rho_0$  is the lateral separation such that the MCF becomes equal to  $1/e$  and is called the lateral coherence length. If  $d > \rho_0$  where  $d$  is the diameter of the aperture, the turbulence along the path of the beam reduces the lateral coherence between different elements of the aperture and effectively transforms it into a partially coherent radiator of dimension,  $\rho_0$ , which decreases with increasing distance from the aperture [13]. But if  $d < \rho_0$ , the entire aperture behaves like a coherent radiator. Thus the resulting field distribution is characteristic of a coherent aperture with a diameter  $d_{\text{eff}}$  equal to the smaller of  $\rho_0$  and  $d$ . Yura [17] showed that if  $L \gg Kd d_{\text{eff}}$ , the beam properties may be approximated by those of a spherical wave and if  $L \ll Kd d_{\text{eff}}$ , the beam properties may be approximated by those of a plane wave.

In the absence of turbulence, a gaussian laser beam will have a far-field angular spread  $\theta = 2\lambda/\pi d$ . When turbulence is present along the path, the scattering of the beam by the moving turbulent eddies causes additional spreading which is greater than  $\theta$  under some conditions.

The spreading of the beam consists of the deflection of the beam as a whole by the eddies larger than the beam diameter  $d$  and by the broadening of the beam due eddies smaller than  $d$ . The separation of the beam spread into the two components of wander and broadening is usually based on the length of the time of observation. If  $V$  is the transverse wind-velocity component, the turbulence eddies are interacting with the beam in time intervals of order  $\Delta t \sim d/V$ . For times much longer than  $\Delta t$ , the received spot will be fully spread due to wander and broadening. The total spot size, viewed on a time scale  $T \gg \Delta t$ , is called the long-term spot size and the beam radius of long-term spread is denoted by  $\rho_L$ . If a picture with an exposure time much less than  $\Delta t$  were taken of the beam, a laser spot of radius  $\rho_s$  broadened by the small eddies at some distance  $\rho_c$  normal to the line of sight would be observed.  $\rho_c$  is the radius of beam-centroidal motion.

The concepts of the beam spread just discussed apply only if the beam is intact. When the beam wander effect is removed, the atmospheric spreading of the beam at the receiver is the short-term beam spread; however, when the turbulence along the path is strong, the beam breaks up into multiple patches and there is not much wander. Kerr and Dunphy [18] found experimentally at near field that the focused beam broke up at the receiver into a proliferation of transmitter-diffraction-scale patches when there is either transmitter misadjustment or strong turbulence. Reidt and Höhn [19] observed in recent experiments that the focused beam at  $0.63 \mu\text{m}$  was broken into several spots of characteristic length  $2\lambda L/\pi d$  which is the free-space diffraction-limited focused radius. They verified also the inverse variation of the patch size with the diameter of the beam, that is, the increase in patch size with decreasing beam diameter or vice versa.

The beam will be quivering while remaining intact as long as the turbulence is relatively weak and the path is not too long or, more precisely, if  $L < L_{\text{CR}}$  where  $L_{\text{CR}}$  is the critical range defined by  $L_{\text{CR}} = K d_{\text{eff}}^2$  where  $d_{\text{eff}}$  is the smaller of  $\rho_0$  and  $d$  [20].

Quantitatively, the spreading of the beam depends on the lateral coherence length  $\rho_0$ . If the beam diameter  $d$  is much smaller than  $\rho_0$ , the effect of turbulence on the beam is negligible and the beam diameter in the far field will be that due to diffraction, namely,  $2\lambda L/\pi d$ . However, if the beam diameter is greater than the lateral coherence length  $\rho_0$ , the beam diameter is given by  $2\lambda L/\pi \rho_0$  [20]. That is, the beam behavior is characteristic of an aperture of diameter  $\rho_0$  instead of  $d$ . The turbulence along the path transforms the aperture into a partially coherent radiator. For the initial field distribution of gaussian form given by

$$U_0(r) = \exp \left[ -\frac{2r^2}{d^2} - \frac{iKr^2}{2F} \right] ,$$

where  $F$  is the radius of the curvature, the long term beam radius is obtained as [21]:

$$\langle \rho_L^2 \rangle \simeq \frac{4L^2}{K^2 d^2} + \frac{d^2}{4} \left( 1 - \frac{L}{F} \right)^2 + \frac{4L^2}{K^2 \rho_0^2} . \quad (16)$$

When the turbulence is strong, the beam will be broken up and for this case Klyatskin and Kon [22] found that the wander of the center of gravity of the beam may be obtained from

$$\langle \rho_c^2 \rangle \approx C_n^{8/5} K^{-1/15} L^{37/15} \quad (17)$$

for constant  $C_n$ ,  $L \gg K\rho_0^2$  (far-field case), and  $d \gg \rho_0$ . Taking the ratio of equations (17) and (16) and observing that the last term on the left hand side of equation (16) is dominant for strong turbulence, we obtain

$$\frac{\langle \rho_c^2 \rangle}{\langle \rho_L^2 \rangle} \sim \left( \frac{K\rho_0^2}{L} \right)^{1/3} \quad (18)$$

Since  $L \gg K\rho_0^2$  then  $\langle \rho_c^2 \rangle \ll \langle \rho_L^2 \rangle$ , which means that the motion of the beam centroid is negligible compared with the beam spread when the beam breaks up into multiple patches. It is not possible to tell how many patches will form, but the bright patches will be in a zone with mean square radius  $\rho_L^2$  [23].

For ranges less than the critical range, tracking laser transmitters have been proposed and discussed [24, 25] to compensate the beam wander which is a relatively low-frequency phenomenon of the order of 0.5 Hz. For  $L < L_{CR}$ , the beam centroidal motion is given approximately by [26]

$$\langle \rho_c^2 \rangle \approx \frac{2.97 L^2}{K^2 \rho_0^{5/3} d^{1/3}} \quad (19)$$

and appears to satisfy a gaussian distribution [27] on each axis.

One of the basic observations on laser beams is the fluctuations in intensity in addition to fluctuations in beam size and position. Fluctuations in intensity are called scintillations. Experimental data on scintillations are extensive at present and are usually expressed as the normalized variance of the intensity:

$$\sigma_I^2 = \frac{\langle I^2 \rangle - \langle I \rangle^2}{\langle I \rangle^2} \quad (20)$$

$I$  is the measured value of the fluctuating intensity and  $\langle I \rangle$  is the average. The statistical theories of optical propagation in a randomly inhomogeneous medium usually calculate the variance in the log-amplitude  $X$ . The log-amplitude  $X(x)$  at any location  $x$  is related to the intensity or the irradiance  $I(x)$  by

$$X(x) = \ln \frac{A}{\langle A \rangle} = \frac{1}{2} \ln \frac{I(x)}{\langle I \rangle} \quad (21)$$

where  $A$  is the amplitude. The variance of the log-amplitude is theoretically given by

$$\sigma_T^2 = 0.124 K^{7/6} L^{11/6} C_n^2, \quad L \gg \frac{\ell_0^2}{\lambda} \quad (22)$$

for a spherical wave. Experiments have confirmed the increase of the log-amplitude variance as the  $11/6$  power of the path length, as the  $7/6$  power of the optical wavenumber  $K$ , and the square of the strength of turbulence for a homogeneous path, i. e.,  $C_n^2$  = constant along the path as long as  $\sigma_T^2 < 0.3$  for the spherical wave [28].

Increase of the path length or the strength of turbulence beyond  $\sigma_T^2 = 0.3$  fails to produce corresponding increase in the measured value of the log-amplitude variance  $\sigma_x^2$  which slows down, reaches a maximum, and begins

to decrease, reaching an asymptotic value of approximately 0.23 independent of wavelength, path length, and parameters of the turbulent medium. Thus the scintillation of an optical beam does not increase indefinitely but tends to saturate for strong turbulence and long paths. This is shown schematically in Figure 2. The more precise way of showing the saturation effect is to plot the theoretical value of log-amplitude variance along the x-axis and the experimental value of the log-amplitude variance on the y-axis, as is usually done in the literature [28].

The probability distribution of the amplitude or intensity fluctuation is an important aspect in optical communications. Theoretically the application of the central limit theorem leads to a normal distribution of the log-amplitude; i. e., the scintillations follow a log-normal distribution. For a unit-amplitude plane wave, the probability density of intensity  $p(I)$  satisfies

$$p(I) = \frac{1}{(2\pi)^{1/2} \sigma I} \exp \left[ - \left( \ln I + \frac{\sigma^2}{2} \right)^2 (2\sigma^2)^{-1} \right]$$

where

$$\sigma^2 = \ln \left( 1 + \sigma_I^2 \right) \quad .$$

For  $\sigma_T^2 \ll 4$ , there is extensive experimental evidence in support of log-normal distribution of intensity. Physically the reason for the log-normal distribution is the multiplicative effect of the refractive-index variations along the path on the intensity [9]; i. e., the field is modulated in each subrange of the path multiplicatively if it is assumed that the effect of atmosphere in each subrange is independent of the degree of coherence. Hence the variation of the logarithm of the amplitude and intensity is the sum of several random variations induced along the path of propagation which leads to a normal distribution due to the central-limit theorem. Experimental measurements by Gracheva, et al. [29] indicate that the log-normal distribution is a reasonable approximation for  $25 < \sigma_T^2 < 100$ . For  $1 \leq \sigma_T^2 \leq 25$ , there are significant deviations from the

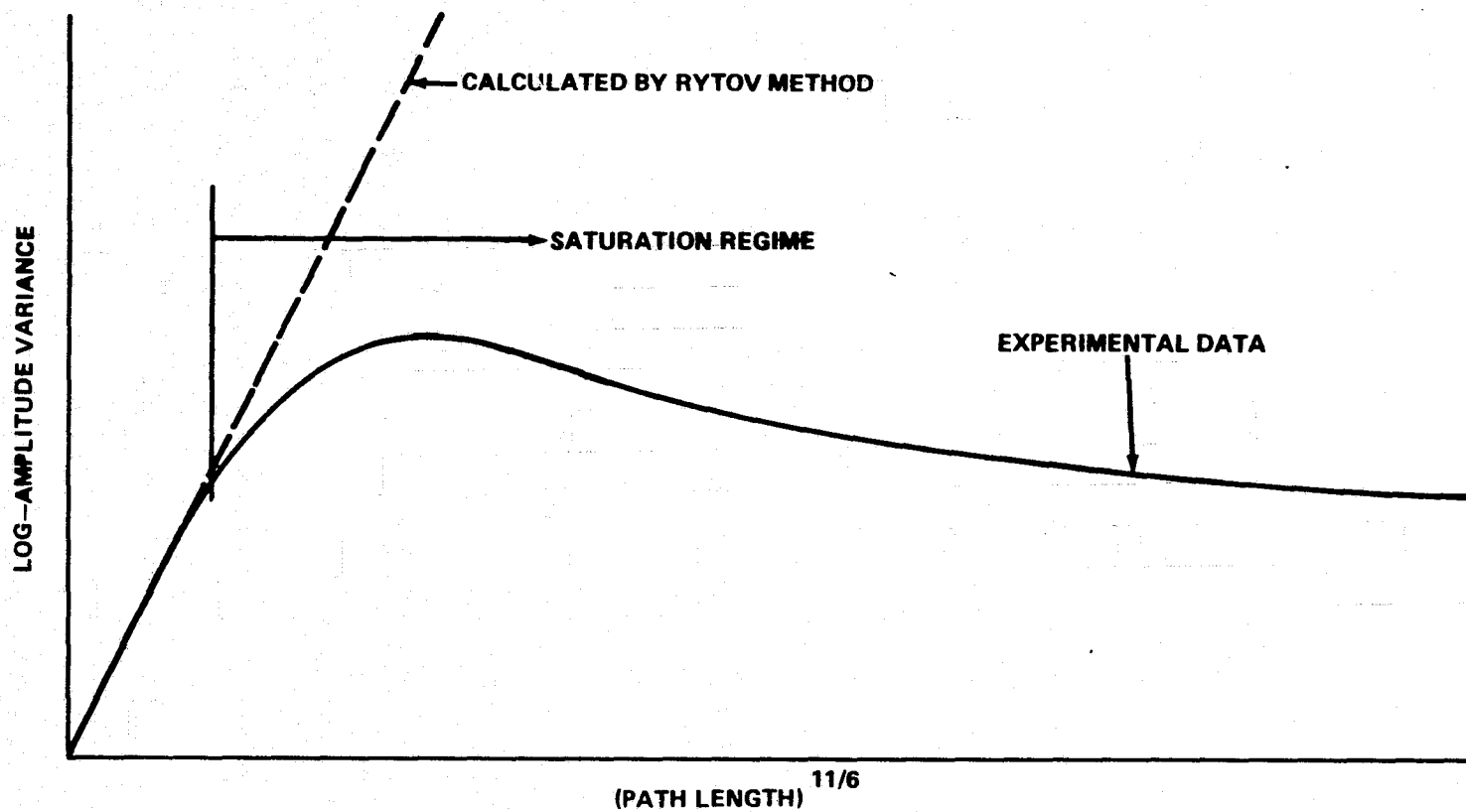


Figure 2. Saturation of the variance of log-amplitude fluctuations of a spherical wave propagating through a homogeneous ( $C_n^2 = \text{const.}$ ) turbulence path.

log-normal distribution. They did not notice Rayleigh distribution, as predicted by de Wolf [30] for large values of  $\sigma_T^2$ . Physically, Rayleigh distribution

results when the field at the receiver is the sum of a large number of independently scattered fields. The physical model of de Wolf [10] attributes the Rayleigh distribution to the multiple scattering by off-axis eddies which are large in strong turbulence.

In addition to temporal variation, the received field exhibits a spatially varying intensity after propagation through turbulence. The spatial structure of scintillations is usually studied by the covariance of the logarithm of the amplitude fluctuations. A correlation length may be defined in several ways. One definition is the value of separation for which the spatial covariance function goes to zero for the first time. The correlation length provides a measure of the separation between two points over which the scintillations are correlated. The concept of the correlation length has been useful for some applications. For example, the theoretical calculation of the log-amplitude variance is usually based on a point detector. In practice, a collector aperture of diameter less than the correlation length is treated as a point detector for comparison of theory and experiment. Another use of the correlation length is in understanding the aperture averaging effect which is discussed later. The intensity covariance function is usually measured and is related to the log-amplitude covariance as [31]

$$C_I(\rho) = \langle I \rangle \left[ \exp \{4 C_X(\rho)\} - 1 \right] \quad (23)$$

where the separation is  $\rho = |x - x'|$ , the covariance of log-amplitude is

$$C_X(\rho) = \langle [X(x) - \langle X \rangle] [X(x') - \langle X \rangle] \rangle ,$$

and the covariance of intensity is

$$C_I(\rho) = \langle [I(x) - \langle I \rangle] [I(x') - \langle I \rangle] \rangle .$$

The intensity and the log-amplitude correlation distances may be seen to be the same from equation (23) but the curves differ greatly. For plane or spherical wave propagation,  $C_X(\rho)$  has the form

$$C_X(\rho) = \sigma_X^2 f\left(\frac{\rho}{(\lambda L)^{1/2}}\right)$$

where  $f$  is a function which depends on the mode of propagation. The first zero of  $f$  is the correlation length and is approximately  $0.76 (\lambda L)^{1/2}$  for a plane wave and  $1.8 (\lambda L)^{1/2}$  for a spherical wave based on the perturbation theory of Tatarski. Experiments confirm a correlation length of the order of  $(\lambda L)^{1/2}$  when there is no saturation of scintillations.

The classical method of reducing the fluctuations in the received power has been to increase the size of the receiving optics. The reduction of the fluctuations in the received power, when the diameter of the receiving aperture is increased, is called aperture averaging. The physical reasoning is that large apertures tend to average over the statistically independent portions of the scintillation pattern [31]. The diameter of an independent patch is usually imagined to be of the order of the correlation length. Thus for weak scintillations, the size of the patch is of the order of the Fresnel length  $(\lambda L)^{1/2}$ . Experiments [32] show that the correlation length decreases as the turbulence gets stronger. Moreover, the covariance curve develops a progressively higher correlation tail and aperture averaging deteriorates as the turbulence strength increases. Figure 3 illustrates the covariance function for several  $\sigma_T^2$ .

To summarize, the phenomenon of saturation of optical scintillation may be characterized by the following experimental observations:

1. There is a physical break-up of the beam into multiple patches when the turbulence is strong.

2. The variance of the log-amplitude reaches a maximum instead of increasing indefinitely and then decreases to an asymptotic value of approximately 0.23 independent of the wavelength of the optical radiation and parameters of the turbulent medium as the path length, or the strength of turbulence, or both are increased.



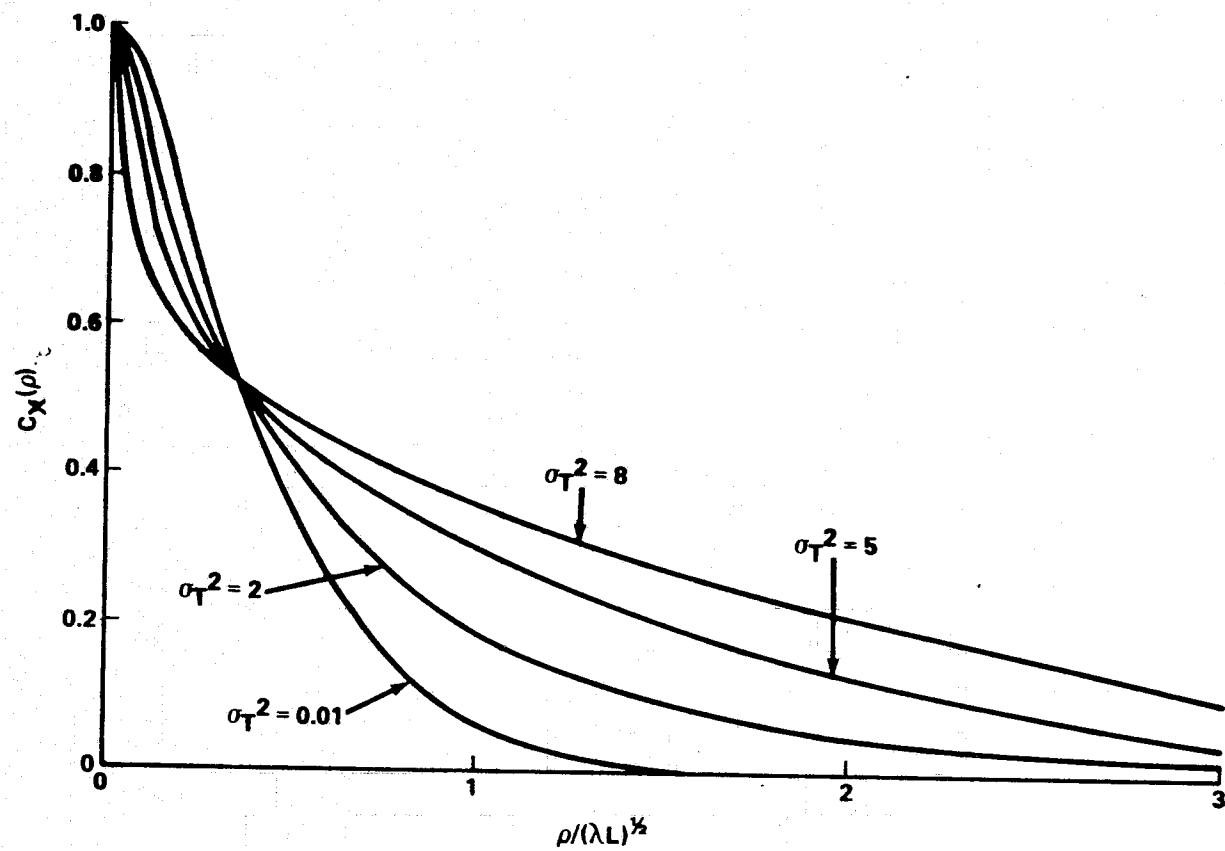


Figure 3. Theoretical curves of the log-amplitude covariance function in weak to strong turbulence [34].

3. The spatial covariance function of log-amplitude decays progressively faster but maintains a progressively higher tail as a function of the detector spacing with increasing turbulence strength and path length.

4. Aperture averaging becomes progressively less effective for a given size of the aperture as the turbulence strength and the path length are increased.

There were several theoretical attempts to explain the saturation phenomenon in the past but it is only in recent years that the theory is able to account for all the observed effects. Since the saturation effect is observed under conditions of strong turbulence, a working definition is needed for the conditions specified as weak or strong turbulence. The turbulence is called "weak" if the theoretical variance of log-amplitude

$$\sigma_T^2 = 0.124 K^{7/6} L^{11/6} C_n^2$$

satisfies the inequality  $\sigma_T^2 < 0.3$ . The turbulence is called "strong" if  $\sigma_T^2 > 0.3$ .

Thus the specification of the turbulence conditions involves not just the refractive-index structure constant  $C_n^2$  but a combination of the wavelength of radiation, path length and  $C_n^2$ .

One of the earlier attempts to physically explain saturation is that by Young [33]. When stellar scintillation is observed with small apertures, the total modulation power first increases with zenith angle and then decreases. Young suggested that the smearing or blurring of the details of the wavefront distortions caused by the intervening atmospheric turbulence is responsible for the observed saturation of astronomical scintillation. The blurring effect is produced by the small-scale fluctuations in the wavefront which change rapidly due to the short lifetime of the small eddies. Thus, a shadow pattern produced by a high layer in the atmosphere becomes smeared or washed out by the intervening turbulence as it propagates down through the atmosphere.

Clifford, Ochs, and Lawrence [34] give a detailed description of the smearing process in the scintillation pattern in strong turbulence. The wavefront develops small-scale and large-scale distortions while passing through the turbulent medium. When such a distorted wave is incident on a Fresnel-zone-size eddy, the small-scale distortions reduce the resolving power of the eddy

while distortions larger than the eddy merely tilt the diffraction pattern of the eddy. The small scale distortions may be expected to change in detail several times during the lifetime of the larger eddies due to the shorter lifetimes of small eddies. These fluctuations of the small-scale distortions of the wavefront cause the smearing of the diffraction pattern of the Fresnel-size eddy, thus making it less effective as a producer of scintillation. Scintillations remain bounded and do not build up indefinitely due to the smearing by the small-scale eddies.

The smearing effect of strong turbulence is incorporated into the first-order analysis by means of a spectral-filter function which filters out higher spatial frequencies. The spectral filter function is given by the normalized two-dimensional Fourier transform of the short term average of the irradiance profile of an optical beam propagating through turbulence. The filter function turns out to be the short term modulation transfer function (MTF). It is assumed that the log-amplitude covariance of a spherical wave for strong turbulence is given by the first-order log-amplitude covariance whose spatial frequency spectrum has been modified by multiplication with the spectral filter function (or the short term MTF). The log-amplitude covariance thus calculated agrees well with the experiments and is shown in Figure 3.

From this covariance function, Clifford and Yura [35] obtained the following asymptotic behavior for the log-amplitude variance:

$$\sigma_X^2 = 0.36 (\sigma_T^2)^{-2/5} + 0.42 \alpha^{5/3} \quad (24)$$

where  $\alpha$  is a constant found from experiments. For  $\alpha = 0.7$ , which is obtained from the strong scintillation data,  $\sigma_X^2$  tends to 0.23 for large values of  $\sigma_T^2$ .

The perturbation theory of Tatarski [7,9] implicitly assumes that the initial coherence is maintained along the propagation path and eddies having scale sizes of the order of the Fresnel length are most effective in producing scintillation. However, as the wave travels through the medium, the transverse spatial coherence decreases continuously and the wave becomes partially coherent. As was previously noted, the spreading of a beam of initial diameter  $d$  in a turbulent medium is characteristic of an aperture of diameter  $\rho_0$  (the lateral coherence length) and not of diameter  $d$ . The radiator has become

partially coherent in the presence of turbulence. Incorporating the loss of coherence of a radiator in the turbulent medium into the analysis, Yura [36] obtained the saturation of scintillations and the behavior of the amplitude covariance. He showed also that in the strong turbulence regime, the amplitude correlation length is equal to the lateral coherence length and  $C_n^2$  increase.

The turbulent eddies most effective in producing scintillations in the saturation regime are those that have scale sizes of the order of the lateral coherence length and not the Fresnel length.

The asymptotic log-amplitude variance behavior of  $(\sigma_T^2)^{-2/5}$  has been predicted also by Fante [37] and Gochelashvily and Shishov [38] from approximate solutions to the equation satisfied by the fourth moment of the field.

The physical theories [34, 35, 36] and the approximate solutions [37, 38] have been able to predict the observed behavior of the covariance function, namely, a rapid fall-off followed by a slow decay resulting in a long tail. These curves indicate that there are small-scale and large-scale structures in the scintillation pattern for strong turbulence. The correlation in strong turbulence is over a transverse separation of the order of

$$\rho_0 \sim \frac{(\lambda L)^{1/2}}{(\sigma_T^2)^{3/5}} .$$

As  $\sigma_T^2$  increases, the lateral coherence length and the amplitude correlation length decrease. The diameter of the detector must be smaller than  $\rho_0$  for point detector performance in strong turbulence.

The aperture averaging which produced a reduction in scintillation noise became less effective for a given aperture of the receiver as the turbulence increased. This effect is due to the presence of large-scale scintillations at the receiver as  $\sigma_T^2$  increased.

Another quantity of interest is the temporal frequency spectrum of intensity fluctuations observed at a fixed point. The width of the frequency spectrum is of the order of  $V/(\lambda L)^{1/2}$  for weak turbulence where  $V$  is the

velocity component normal to the beam. This is typically 10 to 100 Hz. For the case of strong turbulence, the width of the frequency spectrum is of the order  $V/\rho_0$  which is approximately 100 to 1000 Hz. In fact, the peak of the spectrum occurs at approximately  $V/(\lambda L)^{1/2}$  for  $\sigma_T^2 < 1$  and at approximately  $V/\rho_0$  for  $\sigma_T^2 > 1$ .

In addition to the shifting of the peak of the spectrum to higher frequencies, there is a broadening of the spectrum and the maximum value of the spectrum decreases for increasing  $\sigma_T^2$ . These features of the spectrum have been qualitatively observed in the experiments. Finally, to obtain all of the temporal information of the scintillation in the strong turbulence regime, it may be necessary to use an electronic bandwidth of the order of  $V/\rho_0$ . Otherwise, the use of a smaller electronic bandwidth may result in an apparent decrease of the log-amplitude variance for increasing values of  $\sigma_T^2$ .

## V. EFFECT OF TURBULENCE ON HETERODYNE LASER DOPPLER SYSTEMS

In a heterodyne receiver, the incoming wave which is usually weak is combined with a reference wave on the photodetector surface. Coherent detection results from the square-law response of the photodetector to the incident radiation. The squaring operation of the photodetector produces a current at the intermediate frequency which contains the signal-modulation information.

The heterodyne detection of an atmospherically distorted wavefront has been the subject of several studies [39,40]. The various effects of atmospheric turbulence on the laser beam are related to the image behavior in a heterodyne system. Comparison of the expression for the optical power density due to a laser transmitter at a point some distance  $L$  away from the transmitter and the expression for the signal-to-noise ( $S/N$ ) ratio of a heterodyne receiver detecting a signal from a point source at a distance  $L$  shows that they have identical functional dependence on the turbulence parameters. Thus the telescope performance measured in terms of the coherence diameter remains the same whether it is used as part of a transmitter or as part of a heterodyne receiver for propagation in a turbulent atmosphere [41]. In simple terms, the reciprocity between the transmitter and receiver tells that the average target

illumination is related to the power received by the heterodyne receiver. Further, beam wander and beam spread in the target illumination system are related respectively to image dancing and spread in the heterodyne receiver. Thus the beam-image reciprocity implies the familiar effects of turbulence on the beam propagation in the analysis of the heterodyne detection.

Fried [39] considered the amplitude and phase fluctuations and found that for an atmospherically distorted plane wave and a plane-wave local oscillator there is an upper limit to the achievable S/N no matter how large the detector aperture is. The aperture diameter for the near-peak value of S/N is of the order of the lateral coherence diameter. This aperture size has the virtue of avoiding large signal power fluctuations and variance which would result for larger collection apertures. Moreland and Collins [40] tried to determine the possibility of increasing S/N by properly shaping the local oscillator beam and came to the conclusion that, though the optimum local oscillator shape differs significantly from that of a plane wave, the increase of average S/N over the plane-wave case is negligible.

## VI. CALCULATION OF S/N LOSS FOR THE MSFC SYSTEM

The MSFC pulsed laser Doppler system consists of a coherent CO<sub>2</sub> laser operating at 10.6  $\mu\text{m}$  wavelength and transmits 140 pps adjustable in width from 2 to 8  $\mu\text{s}$  through a modified Cassegrain telescope. A homodyne receiver collects the backscattered laser radiation which is detected by an infrared detector and processed in signal-processing electronics. A block diagram of the MSFC system is shown in Figure 4. The transmitted laser beam is assumed to have a gaussian amplitude distribution in the radial direction. The laser beam passes through a telescope with a nominal range of focusing  $f$  from the transmitter.

The wave function at a distance  $L$  from the transmitting telescope of radius  $R$  may be written by the Fresnel diffraction theory in the absence of turbulence along the path as [42-44]

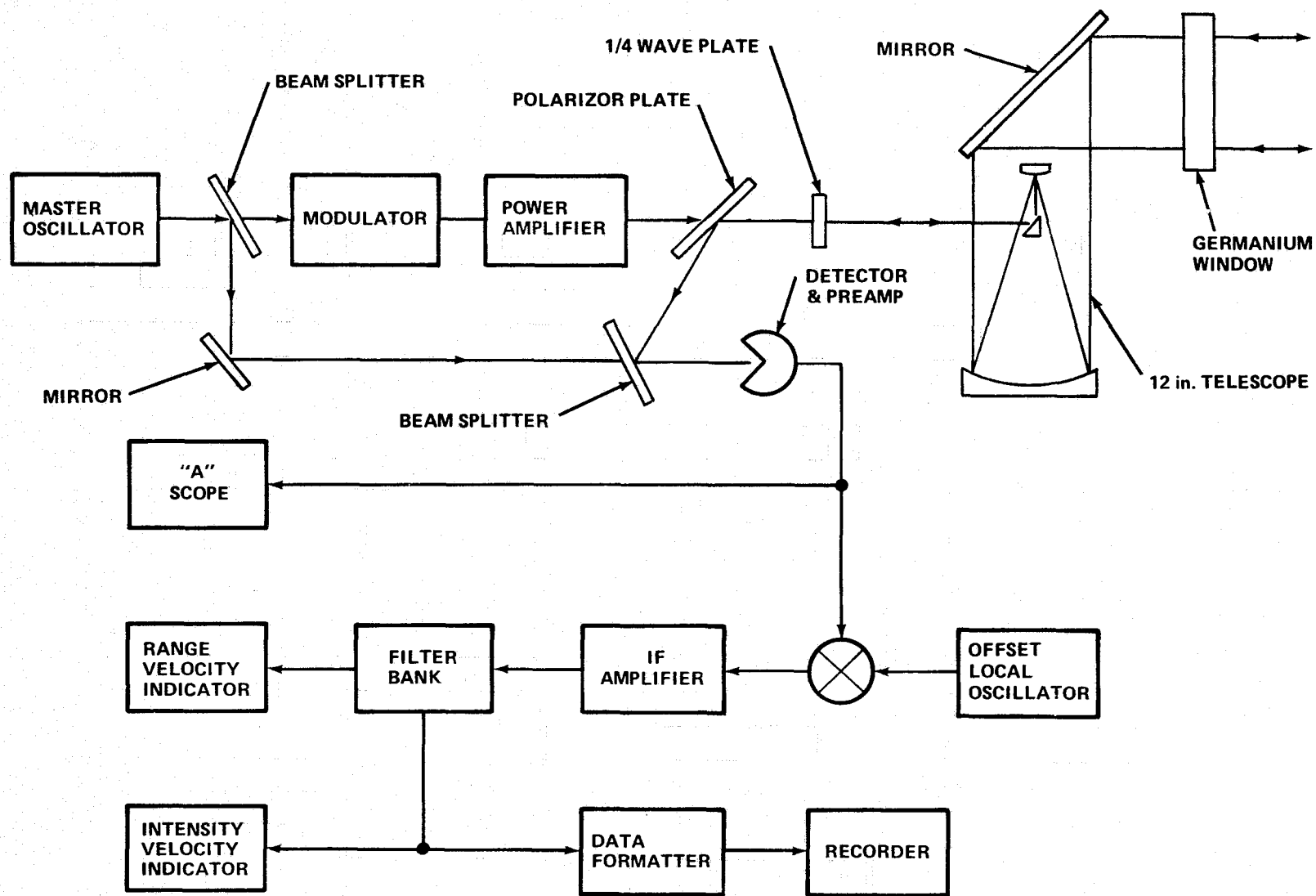


Figure 4. Block diagram of the MSFC pulsed laser Doppler system.

$$\psi(x, y, L) = \left(\frac{2}{\pi}\right)^{1/2} \frac{A}{LR\lambda} [\exp i(KL - \omega t)] \int_{-\infty}^{+\infty} \int_{-\infty}^{+\infty} \exp \left[ i \frac{\pi}{\lambda L} (\vec{r} - \vec{r}'')^2 - i \frac{\pi}{\lambda f} \vec{r}''^2 - \frac{\vec{r}''^2}{R^2} \right] dx'' dy'' , \quad (26)$$

where

$A^2$  = number of photons transmitted per second,

$\vec{r}''$  = vector in the plane of the transmitting lens,

$\vec{r}$  = vector in the plane at distance  $L$  from the transmitter and normal to the optic axis,

$\lambda$  = wavelength of laser radiation,

$\omega$  = angular frequency

$t$  = time.

Equation (26) may be integrated by completing the square and the result is

$$\psi(x, y, L) = \left(\frac{AR}{\lambda L}\right) \left(\frac{2\pi}{1 + \beta^2(1 - \xi^2)}\right)^{1/2} \exp \left[ i(KL - \omega t + \phi) - \frac{(\beta \vec{r})^2}{R^2[1 + \beta^2(1 - \xi^2)]} \right] \quad (27)$$



where

$$\beta = \frac{\pi R^2}{\lambda L} ,$$

$$\xi = \frac{L}{f} ,$$

and

$$\phi = \tan^{-1} [\beta(1 - f)] + \frac{\pi \vec{r}^2}{\lambda L} \frac{1 - \beta^2 \xi (1 - \xi)}{1 + \beta^2 (1 - \xi^2)} .$$

The effect of the atmospheric turbulence along the path of propagation is to produce random variations of phase and intensity. These random variations are introduced into the analysis by multiplying equation (26) with

$$[X(\vec{r}, \vec{r}'') + i S(\vec{r}, \vec{r}'')] .$$

$X(\vec{r}, \vec{r}'')$  is the perturbation of logarithm of amplitude, equation (21), and  $S(\vec{r}, \vec{r}'')$  is the perturbation of phase between the point  $\vec{r}''$  at the transmitter and the range point  $\vec{r}$ . Thus the outgoing wave function at a distance  $L$  with the effect of turbulence is given by

$$\begin{aligned} \psi(x, y, L) = & \left( \frac{2}{\pi} \right)^{1/2} \frac{A}{LR\lambda} \exp [i(KL - \omega t)] \int_{-\infty}^{\infty} \int_{-\infty}^{\infty} \exp \left[ i \frac{\pi}{\lambda L} (\vec{r} - \vec{r}'')^2 \right. \\ & \left. - i \frac{\pi}{\lambda f} \vec{r}''^2 + i S(\vec{r}, \vec{r}'') + X(\vec{r}, \vec{r}'') - \frac{\vec{r}''^2}{R^2} \right] dx'' dy'' . \quad (28) \end{aligned}$$

The transmitted wave is assumed to be backscattered by a diffuse target of scattering particles. Considering a single particle, the incoming wave is scattered by the particle as a spherical wave, and the scattered wave function at a point  $\vec{r}'$  in the plane of the receiving lens for a coaxial system is given by

$$\psi_s(\vec{r}') = \left( \frac{\sigma'}{4\pi L^2} \right)^{1/2} \psi(\vec{r}) \exp \left\{ -i \left[ \frac{\pi}{\lambda f} \vec{r}'^2 - \frac{\pi}{\lambda L} (\vec{r} - \vec{r}')^2 - (KL + \Delta\omega t) - S(\vec{r}, \vec{r}') \right] + X(\vec{r}, \vec{r}') \right\} \quad (29)$$

where

$\sigma'$  = backscattering coefficient of the particle,

$\Delta\omega = 2\omega V/c$  = Doppler shift due to the velocity component  $V$  of the moving particle along the optic axis,

$X(\vec{r}, \vec{r}')$  = perturbation of the log-amplitude, and

$S(\vec{r}, \vec{r}')$  = perturbation of phase, between the range point  $\vec{r}$  and the point  $\vec{r}'$  at the receiver.

The local oscillator reference wave function which is added to the received wave function is assumed a plane wave with gaussian amplitude variation which may be written as

$$\psi_{\text{ref}} = \alpha A \exp \left( -i\omega t - \frac{\vec{r}'^2}{R^2} \right) \quad (30)$$

where  $\alpha$  is a constant and the arbitrary phase factor is assumed to be zero.

The total signal photo-current is given by the real part of

$$i_s = 2\eta \int_{A_R} \psi_s \psi_{\text{ref}}^* W(\mathbf{r}') d\mathbf{r}' \quad , \quad (31)$$

where  $W(\mathbf{r}')$  is the apodization or transmission function for the receiver aperture and is assumed equal to unity over the width of the reference beam.

Substitution of equations (28), (29), and (30) into equation (31) gives the signal current as the real part of

$$i_s = \frac{\sqrt{2\sigma^2} \alpha A^2 \eta}{\pi L^2 R \lambda} \iint \exp \left[ - \left\{ \frac{\vec{r}'^2}{R^2} + \frac{\vec{r}''^2}{R^2} \right\} + i \left\{ \Delta \omega t + \phi(\vec{r}'', \vec{r}', \vec{r}) + S(\vec{r}, \vec{r}'') + S(\vec{r}, \vec{r}') \right\} + X(\vec{r}, \vec{r}'') + X(\vec{r}, \vec{r}') \right] d\vec{r}' d\vec{r}'' \quad (32)$$

where

$$\phi(\vec{r}, \vec{r}', \vec{r}'') = 2KL + \frac{\pi}{\lambda L} \left[ (\vec{r} - \vec{r}')^2 + (\vec{r} - \vec{r}'')^2 \right] - \frac{\pi}{\lambda f} (\vec{r}'^2 + \vec{r}''^2) \quad .$$

The photo-current due to a single scatterer may be written as

$$i_s = \frac{\sqrt{2\sigma^2} \alpha A^2 \eta}{\pi L^2 R \lambda} \iint \exp \left[ - \left\{ \frac{\vec{r}'^2}{R^2} + \frac{\vec{r}''^2}{R^2} \right\} + X(\vec{r}, \vec{r}') + X(\vec{r}, \vec{r}'') \right] \cos \left[ \Delta \omega t + \phi(\vec{r}'', \vec{r}', \vec{r}) + S(\vec{r}, \vec{r}') + S(\vec{r}, \vec{r}'') \right] d\vec{r}' d\vec{r}'' \quad .$$

The signal power is proportional to  $i_s^2$  and

$$\begin{aligned}
i_s^2 &= \frac{2\sigma^2 \alpha^2 A^4 \eta^2}{\pi^2 L^4 R^2 \lambda^2} \iiint \exp \left[ - \left\{ \frac{\vec{r}^2 + \vec{r}'^2 + \vec{r}''^2 + \vec{r}'''^2}{R^2} \right\} \right. \\
&\quad + X(\vec{r}, \vec{r}') + X(\vec{r}, \vec{r}'') + X(\vec{r}, \vec{r}''') + X(\vec{r}, \vec{r}''') \left. \right] \cos \left[ \Delta \omega t \right. \\
&\quad + \phi(\vec{r}', \vec{r}', \vec{r}) + S(\vec{r}, \vec{r}') + S(\vec{r}, \vec{r}'') \left. \right] \cos \left[ \Delta \omega t \right. \\
&\quad + \phi(\vec{r}''', \vec{r}''', \vec{r}) + S(\vec{r}, \vec{r}''') + S(\vec{r}, \vec{r}''') \left. \right] d\vec{r}' d\vec{r}'' d\vec{r}''' d\vec{r}'''' \\
&= \frac{\sigma^2 \alpha^2 A^4 \eta^2}{\pi^2 L^4 R^2 \lambda^2} \iiint \exp \left[ - \frac{\vec{r}^2 + \vec{r}'^2 + \vec{r}''^2 + \vec{r}'''^2}{R^2} + X(\vec{r}, \vec{r}') \right. \\
&\quad + X(\vec{r}, \vec{r}'') + X(\vec{r}, \vec{r}''') + X(\vec{r}, \vec{r}''') \left. \right] \left\{ \cos \left[ 2\Delta \omega t \right. \right. \\
&\quad + \phi(\vec{r}', \vec{r}', \vec{r}) + \phi(\vec{r}''', \vec{r}''', \vec{r}) + S(\vec{r}, \vec{r}') + S(\vec{r}, \vec{r}'') \\
&\quad + S(\vec{r}, \vec{r}''') + S(\vec{r}, \vec{r}''') \left. \right] + \cos \left[ \phi(\vec{r}', \vec{r}', \vec{r}) + S(\vec{r}, \vec{r}') \right. \\
&\quad + S(\vec{r}, \vec{r}'') - \phi(\vec{r}''', \vec{r}''', \vec{r}) - S(\vec{r}, \vec{r}''') \\
&\quad \left. \left. - S(\vec{r}, \vec{r}''') \right] \right\} d\vec{r}' d\vec{r}'' d\vec{r}''' d\vec{r}'''' .
\end{aligned}$$

If the signal power is averaged over a period longer than  $1/(2\Delta\omega)$ , then

$$\begin{aligned}
i_s^2 &= \text{Re} \frac{\sigma^2 \alpha^2 A^4 \eta^2}{\pi^2 L^4 R^2 \lambda^2} \iiint \exp \left[ - \frac{\vec{r}^2 + \vec{r}'^2 + \vec{r}''^2 + \vec{r}'''^2}{R^2} + X(\vec{r}, \vec{r}') \right. \\
&\quad + X(\vec{r}, \vec{r}'') + X(\vec{r}, \vec{r}''') + X(\vec{r}, \vec{r}''') \left. \right] \exp \left\{ \left[ \phi(\vec{r}', \vec{r}', \vec{r}) \right. \right. \\
&\quad - \phi(\vec{r}''', \vec{r}''', \vec{r}) + S(\vec{r}, \vec{r}') + S(\vec{r}, \vec{r}'') - S(\vec{r}, \vec{r}''') \\
&\quad \left. \left. - S(\vec{r}, \vec{r}''') \right] \right\} d\vec{r}' d\vec{r}'' d\vec{r}''' d\vec{r}''''
\end{aligned}$$

where  $\text{Re}$  denotes the real part. The point  $\vec{r}''$  lies on the receiver aperture and  $\vec{r}'''$  lies on the transmitting aperture.

The expected value of the signal power is obtained by taking the ensemble average of  $i_s^2$  as given by

$$\begin{aligned} \langle i_s^2 \rangle = & \text{Re} \frac{\sigma^2 a^2 A^4 \eta^2}{\pi^2 L^4 R^2 \lambda^2} \iiint \exp \left[ - \frac{\vec{r}''^2 + \vec{r}'''^2 + \vec{r}'''^2 + \vec{r}''''^2}{R^2} \right. \\ & + i \left\{ \phi(\vec{r}'', \vec{r}', \vec{r}) - \phi(\vec{r}''', \vec{r}''', \vec{r}) \right\} \left\langle \exp \left[ \left\{ X(\vec{r}, \vec{r}') \right. \right. \right. \\ & + X(\vec{r}, \vec{r}''') + X(\vec{r}, \vec{r}'') + X(\vec{r}, \vec{r}''') \left. \right\} + i \left\{ S(\vec{r}, \vec{r}') + S(\vec{r}, \vec{r}'') \right. \\ & \left. \left. \left. + S(\vec{r}, \vec{r}''') - S(\vec{r}, \vec{r}''') \right\} \right] \right\rangle d\vec{r}' d\vec{r}'' d\vec{r}''' d\vec{r}'''' . \quad (33) \end{aligned}$$

It is assumed that the outgoing and incoming paths are statistically independent. This assumption allows the following:

$$\begin{aligned} \left\langle \exp \left[ \left\{ X(\vec{r}, \vec{r}') + X(\vec{r}, \vec{r}''') \right\} + i \left\{ S(\vec{r}, \vec{r}') - S(\vec{r}, \vec{r}''') \right\} \right. \right. \\ \left. \left. + \left\{ X(\vec{r}, \vec{r}'') + X(\vec{r}, \vec{r}''') \right\} + i \left\{ S(\vec{r}, \vec{r}'') \right. \right. \right. \\ \left. \left. \left. - S(\vec{r}, \vec{r}''') \right\} \right] \right\rangle = \exp \left[ - \frac{1}{2} \left\{ D(|\vec{r}' - \vec{r}'''|) \right. \right. \\ \left. \left. + D(|\vec{r}'' - \vec{r}'''|) \right\} \right] \end{aligned}$$

where  $D(r)$  is the wave structure function. Kolmogorov theory of isotropic turbulence gives a 5/3-power variation for the wave structure function:

$$D(r) = \left( \frac{r}{r_a} \right)^{5/3}$$

where  $r_a$  is proportional to the coherence radius and has the value

$$r_a = 0.05972 \lambda^{6/5} L^{-3/5} C_n^{-6/5}, \quad \text{for plane wave}$$

$$= 0.1047 \lambda^{6/5} L^{-3/5} C_n^{-6/5}, \quad \text{for spherical wave}.$$

It will be appropriate to use  $r_a$  for a spherical wave for the wave originating at the range point.

To simplify the calculations, the structure function is approximated as

$$D(r) = \left( \frac{r}{r_a} \right)^2$$

and the plane-wave value of  $r_a$  is used for both ways to give a conservative estimate.

The expected value of  $i_s^2$  becomes

$$\begin{aligned} \langle i_s^2 \rangle = & \operatorname{Re} \frac{\sigma^2 \alpha^2 A^4 \eta^2}{\pi L^4 R^2 \lambda^2} \iiint \exp \left[ - \frac{\vec{r}^2 + \vec{r}'^2 + \vec{r}''^2 + \vec{r}'''^2}{R^2} \right. \\ & - \frac{1}{2} \frac{|\vec{r}' - \vec{r}''|^2}{r_a^2} - \frac{1}{2} \frac{|\vec{r}'' - \vec{r}'''|^2}{r_a^2} + i \left\{ \phi(\vec{r}', \vec{r}'', \vec{r}) \right. \\ & \left. \left. - \phi(\vec{r}''', \vec{r}'', \vec{r}) \right\} \right] d\vec{r}' d\vec{r}'' d\vec{r}''' d\vec{r}''' \quad (34) \end{aligned}$$

Performing the integrations approximately, the expected value of SNR for a single scatterer is obtained as [42]

$$\langle \text{SNR} \rangle = \frac{\eta A^2 \sigma^2 \pi R^4 \tau}{L^4 \lambda^2 [1 + a^2 + \beta^2 (1 - \xi^2)]^2} \exp \left[ \frac{-4 \left( \frac{\beta r}{R} \right)^2}{1 + a^2 + \beta^2 (1 - \xi^2)} \right] \quad (35)$$

where  $a = (R/r_a)$  and  $\tau$  is the pulse duration. Integrating equation (35) over a plane normal to the axis at the range  $L$ , the S/N ratio due to a plane target (dropping the angle brackets) is obtained:

$$\frac{S}{N} = \frac{\eta \sigma^2 \tau R^2 A^2}{4 \left[ L^2 (1 + a^2) + \frac{\pi R^4}{\lambda^2 f^2} (f - L)^2 \right]} \quad (36)$$

In the absence of the turbulence effects,  $a = 0$  and thus the S/N is reduced by the ratio

$$P = \frac{L^2 (1 + a^2) + \frac{\pi^2 R^4}{\lambda^2 f^2} (f - L)^2}{L^2 + \frac{\pi^2 R^4}{\lambda^2 f^2} (f - L)^2} \quad (37)$$

due to turbulence. If the system is focused to infinity, then

$$P = \frac{L^2 (1 + a^2) + \frac{\pi^2 R^4}{\lambda^2}}{L^2 + \frac{\pi^2 R^4}{\lambda^2}} \quad (38)$$

Thus the calculation of the loss of power due to turbulence reduces to the calculation of  $a = R/r_a$  and  $P$ .

The wave structure function for a plane wave is given by

$$D(r) = 2.91 \left( \frac{2\pi}{\lambda} \right)^2 r^{5/3} \int_{\text{Path}} C_n^2 dL \quad (39)$$

For a propagation path which is inclined at an angle  $\theta'$  with respect to the horizontal,

$$h = H + L \sin \theta' \quad (40)$$

where  $h$  is any altitude above sea level and  $H$  is the altitude of the scattering surface above sea level. For flights at Edwards Air Force Base, the dry lake is approximately 600 m above sea level. The strength of turbulence is assumed to vary as

$$C_n^2 = C_{n0}^2 (h')^{-1/3} \exp \left( -\frac{h'}{h_0} \right) \quad (41)$$

where  $C_{n0}^2$  is a constant,  $h' = h - H$ , and  $h_0 = 3200$  m. The value of  $C_{n0}^2$ , obtained from earlier measurements of Huffnagel and Stanley [39,45], is  $4.2 \times 10^{-14}$ . We use  $H = 600$  m and assume that equation (41) is valid from  $h = 10$  m. Substituting equation (41) into equation (39), the structure function may be written as

$$D(r) = 3.38 \times 10^4 C_{n0}^2 r^{5/3} \frac{\operatorname{cosec} \theta'}{\lambda^2} [I(\ell_2) - I(\ell_1)] \quad (42)$$

where  $I(\ell)$  is the incomplete gamma function given by

$$\Gamma\left(\frac{2}{3}\right) I(\ell) = \int_0^\ell u^{-1/3} e^{-u} du, \quad \ell = \frac{h - H}{h_0}$$

and  $\ell_1$  and  $\ell_2$  are dimensionless lower and upper altitudes. From equation (42)



$$r_a = \left[ 3.38 \times 10^4 C_{n0}^2 \frac{\operatorname{cosec} \theta}{\lambda^2} \left\{ I(\ell_2) - I(\ell_1) \right\} \right]^{-3/5}$$

For the flight tests,  $\theta = 7^\circ$  and  $\lambda = 10.6 \mu\text{m}$ . Using these values,  $r_a$  becomes

$$r_a = 5.8 \times 10^{-10} \left[ C_{n0}^2 \left\{ I(\ell_2) - I(\ell_1) \right\} \right]^{-3/5} \quad (43)$$

The optics diameter is taken as 25.4 cm and this gives  $R = 0.127 \text{ m}$ ; therefore,

$$a = \frac{R}{r_a} = 2.19 \times 10^8 \left[ I(\ell_2) - I(\ell_1) \right]^{3/5} C_{n0}^{6/5} \quad (44)$$

The incomplete gamma functions may be obtained from the Pearson Tables [46].

The calculations are made for the flight tests between 600 m and 4000 m altitude and for  $C_{n0}^2 = 4.2 \times 10^{-14}$ . The calculated S/N values shown in Figure 5, also include the transmission loss taken from Reference 5.

The loss due to the atmospheric turbulence is smaller than that due to absorption at  $10.6 \mu\text{m}$  wavelength. As observed in Reference 5, the absorption loss will be least at the DF (deuterium fluoride) laser wavelength,  $3.9 \mu\text{m}$ , but the turbulence loss may be higher due to the smaller lateral coherence diameter.

A comparison of the losses due to absorption and turbulence over a 20 km horizontal path at altitudes of 2.5 km and 5 km is given in Table 1 at  $\text{CO}_2$  and DF laser wavelengths using the same optic size. Due to the smaller coherence diameter at DF wavelength, the optics diameter should be less than that at  $\text{CO}_2$  wavelength. By using the same optics size for both, the turbulence losses have been overestimated for the DF laser. Even so, the total loss for DF system is approximately 15 dB less than for  $\text{CO}_2$  system at 2.5 km. At 5 km altitude, the magnitude of the losses has dropped and there is an improvement of only 5 dB using the DF system. For altitudes below 5 km, the DF system is seen to give less total loss due to the atmosphere.

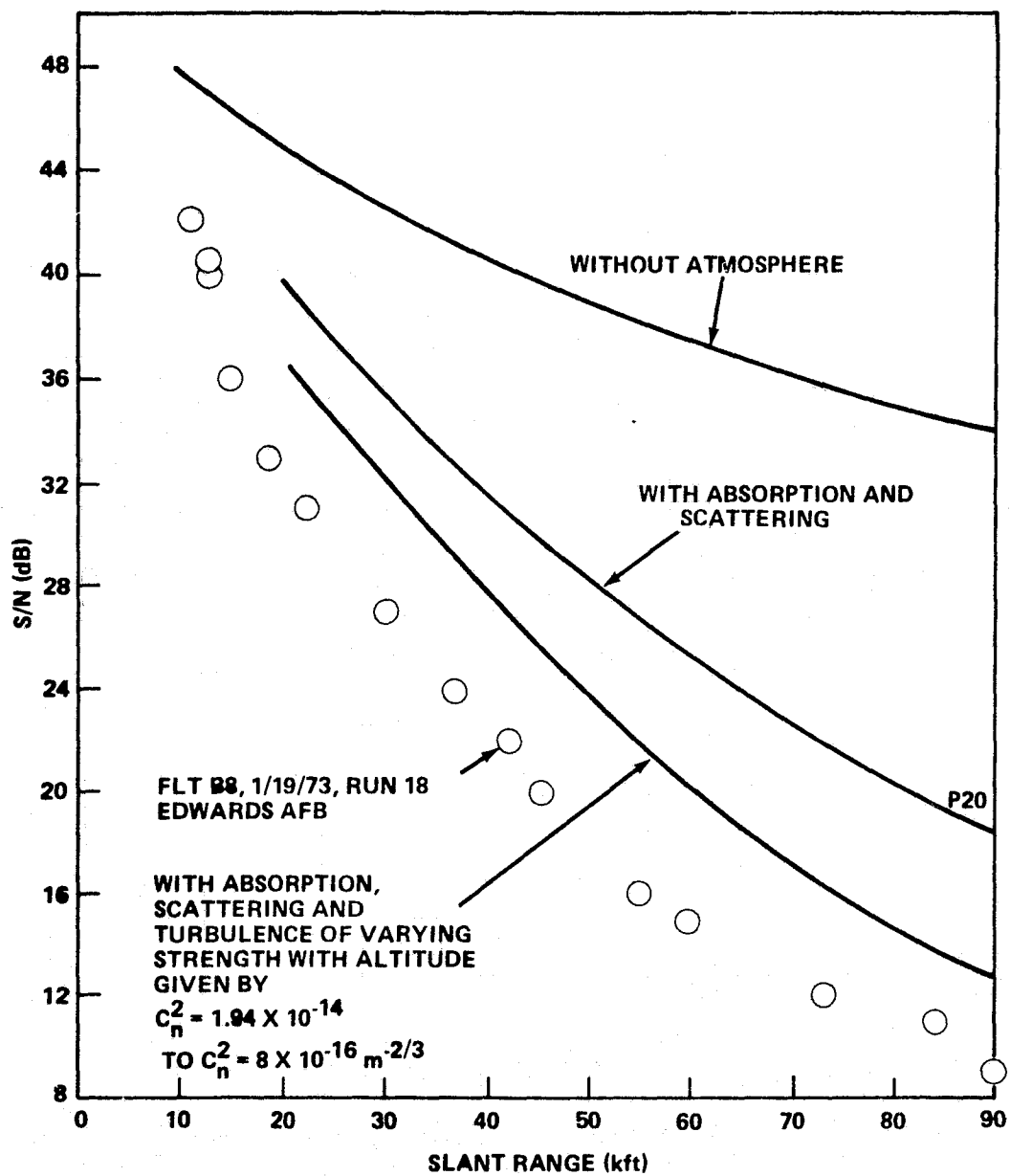


Figure 5. Comparison of measured and theoretical S/N values.

**TABLE 1. COMPARISON OF LOSSES AT CO<sub>2</sub> AND DF LASER  
WAVELENGTHS OVER A 20 km HORIZONTAL PATH  
AT 2.5 km AND 5 km ALTITUDES**

Altitude	Laser	Absorption Loss (dB)	Turbulence Loss (dB)	Total Loss (dB)
2.5 km	CO <sub>2</sub>	24	2.6	26.6
	DF	1.75	9.05	10.8
5 km	CO <sub>2</sub>	9.6	0.37	10.0
	DF	0.46	4.9	5.4

Since the atmospheric conditions are constantly changing, it is desirable to estimate the maximum and minimum attenuation of the CO<sub>2</sub> laser radiation that may be expected due to the atmospheric propagation. The upper limit on the attenuation is estimated using the AFCRL Midlatitude Summer Hazy Atmosphere and an exponential variation with altitude of the turbulence strength with  $C_{n0}^2 = 4.2 \times 10^{-14} \text{ m}^{-2/3}$ . The lower limit on the attenuation is estimated using AFCRL Midlatitude Winter Clear Atmosphere and an exponential variation with altitude of the turbulence strength with  $C_{n0}^2 = 4.2 \times 10^{-15} \text{ m}^{-2/3}$ . The results for a two-way horizontal path of 20 km range at each altitude up to 10 km altitude are shown in Figure 6. The difference in the upper and lower limits of attenuation is considerable near sea level mainly because of the differences in the temperature, humidity, and aerosol concentration. The breakup of the attenuation into the transmission part and turbulence part at each altitude is given in Table 2.

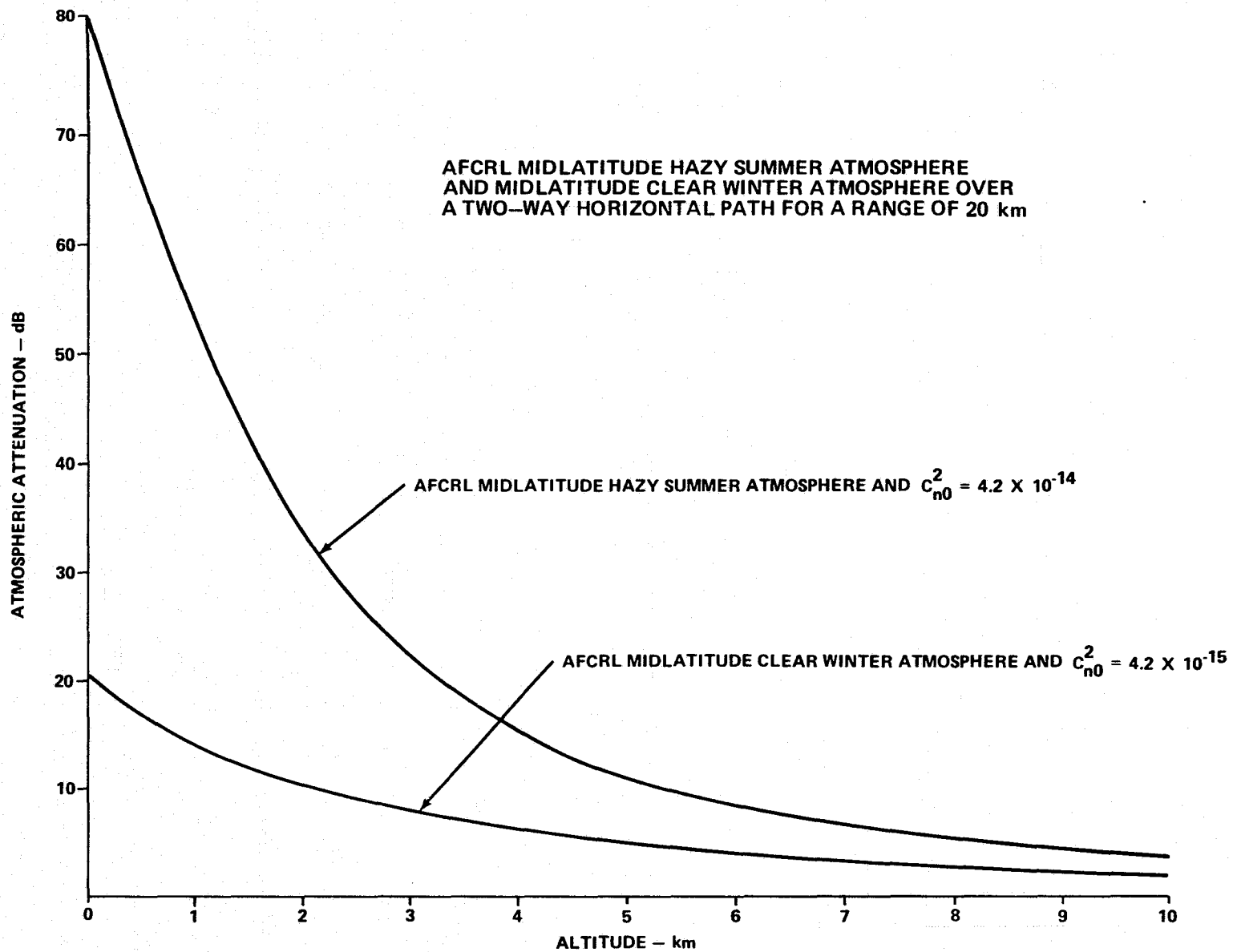


Figure 6. Atmospheric attenuation at  $10.6 \mu\text{m}$ .

**TABLE 2. SIGNAL LOSS IN ATMOSPHERIC PROPAGATION  
AT 10.6  $\mu\text{m}$  DUE TO ABSORPTION, SCATTERING  
AND COHERENCE DEGRADATION FOR A TWO-WAY  
HORIZONTAL PATH OF 20 km AT EACH ALTITUDE**

(a) AFCRL Midlatitude Summer Hazy Atmosphere and $C_{n0}^2 = 4.2 \times 10^{-14}$			
Altitude	Absorption and Scattering Loss (dB)	Turbulence Loss (dB)	Total Loss (dB)
10.0 m	68.0	13.0	81.0
2.5 km	24.6	2.6	27.2
5.0 km	9.6	1.05	10.65
7.5 km	5.8	0.34	6.14
10.0 km	3.53	0.12	3.65
(b) AFCRL Midlatitude Winter Clear Atmosphere and $C_{n0}^2 = 4.2 \times 10^{-15}$			
10 m	17.3	3.4	20.7
2 km	10.5	0.3	10.8
4 km	6.5	-	6.5
7 km	3.5	-	3.5
10 km	1.8		1.8

## VII. CONCLUSIONS

The attenuation of the  $\text{CO}_2$  laser radiation due to absorption, scattering, and turbulence of the atmosphere is estimated for the January 1973 flight test conditions. The theoretical values of S/N including the atmospheric attenuation compare favorably with the flight test results.

The upper and lower limits on the atmospheric attenuation at each altitude up to 10 km may be read from Figure 6 for a two-way horizontal path of 20 km range. These calculations are based on the currently accepted models of atmospheric pressure, temperature, humidity, aerosol concentration, and turbulence strength. These results are expected to be useful in the interpretation of the future test results at several altitudes using the pulsed CO<sub>2</sub> laser Doppler system.

## REFERENCES

1. Huffaker, R. M.: Laser Doppler Systems for Gas Velocity Measurements. Applied Optics, vol. 9, May 1970, p. 1026.
2. Huffaker, R. M.; Jelalian, A. V.; and Thomson, J. A. L.: Laser Doppler Systems for Detection of Aircraft Trailing Vortices. Proceedings of the IEEE, vol. 58, March 1970, p. 322.
3. Huffaker, R. M.: CO<sub>2</sub> Laser Doppler Systems for the Measurement of Atmospheric Winds and Turbulence. Atmospheric Technology, National Center for Atmospheric Research, Winter 1974-1975, p. 71.
4. Huffaker, R. M. et al.: Development of a Laser Doppler System for the Detection, Tracking and Measurement of Aircraft Wake Vortices. NASA TM X-66868, March 1975.
5. Murty, S. S. R.: Atmospheric Transmission of CO<sub>2</sub> Laser Radiation With Application to Laser Doppler Systems. NASA TM X-64987, November 1975.
6. Meyer-Arendt, J. R. and Emmanuel, C. B.: Optical Scintillation; A Survey of Literature. National Bureau of Standards, Technical Note 225, April 5, 1965.
7. Tatarski, V. I.: Wave Propagation in a Turbulent Medium. McGraw-Hill Company, New York, 1961.
8. Kerr, J. R.: Experiments on Turbulence Characteristics and Multi-wavelength Scintillation Phenomena. J. of the Optical Society of America, vol. 62, September 1972, p. 1040.
9. Tatarski, V. I.: The Effects of the Turbulent Atmosphere on Wave Propagation. U.S. Department of Commerce, National Technical Information Service, Springfield, Virginia, 1971.
10. De Wolf, D. A.: Waves in Turbulent Air: A Phenomenological Model. Proceedings of the IEEE, vol. 57, April 1969, p. 375.

## REFERENCES (Continued)

11. Young, A. T.: Aperture Filtering and Saturation of Scintillation. J. Optical Society of America, vol. 60, February 1970, p. 248.
12. Lee, R. W. and Harp, J. C.: Weak Scattering in Random Media, With Applications to Remote Probing. Proceedings of the IEEE, April 1969, p. 375.
13. Davis, J. I.: Consideration of Atmospheric Turbulence in Laser System Design. Applied Optics, vol. 5, January 1966.
14. Lutomirski, R. F. and Yura, H. T.: Propagation of a Finite Optical Beam in an Inhomogeneous Medium. Applied Optics, vol. 10, July 1971, p. 1652.
15. Fante, R.: Mutual Coherence Function and Frequency Spectrum of a Laser Beam Propagating Through Atmospheric Turbulence. J. Optical Society of America, vol. 64, May 1974, p. 592.
16. Fried, D. L.: Limiting Resolution Looking down through the Atmosphere. J. Optical Society of America, vol. 56, October 1966, p. 1380.
17. Yura, H. T.: Mutual Coherence Function of a Finite Cross Section Optical Beam Propagating in a Turbulent Medium. Applied Optics, vol. 11, June 1972, p. 1399.
18. Kerr, J. R. and Dunphy, J. R.: Experimental Effects of Finite Transmitter Apertures on Scintillations. J. Optical Society of America, vol. 63, January 1973, p. 1.
19. Raidt, H. and Höhn, D. H.: Instantaneous Intensity Distribution in a Focussed Laser Beam at 0.63 m and 10.6 m Propagating through the Atmosphere. Applied Optics, vol. 14, November 1975.
20. Yura, H. T.: Short-Term Average Optical Beam Spread in a Turbulent Medium. J. Optical Society of America, vol. 63, May 1973, p. 567.



## REFERENCES (Continued)

21. Yura, H. T.: Atmospheric Turbulence Induced Laser Beam Spread. *Applied Optics*, vol. 10, December 1971, p. 2771.
22. Klyatskin, V. and Kon, A.: On the Displacement of Spatially-Bounded Light Beams in a Turbulent Medium in the Markovian-Random-Process Approximation. *Radiophysics and Quantum Electronics*, vol. 15, September 1972, p. 1056.
23. Fante, Ronald L.: Electromagnetic Beam Propagation in Turbulent Media. *Proceedings of the IEEE*, vol. 63, December 1975, p. 1669.
24. Dunphy, J. R. and Kerr, J. R.: Atmospheric Beam-Wander Cancellation by a Fast-Tracking Transmitter. *J. Optical Society of America*, vol. 64, July 1974, p. 1015.
25. Sher, Lawrence: Tracking Systems Requirements for Atmospheric Steering Compensation. *Applied Optics*, vol. 14, November 1975, p. 2750.
26. Andreev, G. A. and Gel'fer, E. I.: Angular Random Walks of the Center of Gravity of the Cross Section of a Diverging Light Beam. *Radiophysics and Quantum Electronics*, vol. 14, 1971, p. 1145.
27. Fried, D. L.: Statistics of Laser Beam Fade Induced by Pointing Jitter. *Applied Optics*, vol. 12, February 1973, p. 422.
28. Kleen, R. H. and Ochs, G. R.: Measurements of the Wavelength Dependence of Scintillation in Strong Turbulence. *J. Optical Society of America*, vol. 60, December 1970, p. 1695.
29. Gracheva, M.; Gurvich, A.; Kashkarov, S.; and Pokasov, V.: Similarity Correlations and their Experimental Verification in the Case of Strong Intensity Fluctuations of Laser Radiation. *Soviet Physics JETP*, vol. 40, no. 6, 1975, p. 1011.
30. De Wolf, D. A.: Saturation of Irradiance Fluctuations due to Turbulent Atmosphere. *J. Optical Society of America*, vol. 58, April 1968, p. 461.

## REFERENCES (Continued)

31. Fried, D. L.: Aperture Averaging of Scintillations. J. Optical Society of America, vol. 57, February 1967, p. 169.
32. Dunphy, J. R. and Kerr, J. R.: Scintillation Measurements for Large Integrated Path Turbulence. J. Optical Society of America, vol. 63, August 1973, p. 981.
33. Young, A. T.: Saturation of Scintillations. J. Optical Society of America, vol. 60, November 1970, p. 1495.
34. Clifford, S. F.; Ochs, G. R.; and Lawrence, R. S.: Saturation of Optical Scintillation by Strong Turbulence. J. Optical Society of America, vol. 64, February 1974, p. 148.
35. Clifford, S. F. and Yura, H. T.: Equivalence of Two Theories of Strong Optical Scintillation. J. Optical Society of America, vol. 64, December 1974, p. 1641.
36. Yura, H. T.: Physical Model for Strong Optical-Amplitude Fluctuations in a Turbulent Medium. J. Optical Society of America, vol. 64, January 1974, p. 59.
37. Fante, R.: Electric Field Spectrum and Intensity Covariance of a Wave in a Random Medium. Radio Science, vol. 10, January 1975, p. 77.
38. Gochelashvili, K. and Shishov, V.: Saturated Intensity Fluctuations of Laser Radiation in a Turbulent Medium. Soviet Physics JETP, vol. 39, no. 4, October 1974, p. 605.
39. Fried, D. L.: Optical Heterodyne Detection of an Atmospherically Distorted Signal Wave Front. Proceedings of the IEEE, vol. 55, January 1967, p. 57.
40. Moreland, J. P. and Collins, S. A., Jr.: Optical Heterodyne Detection of a Randomly Distorted Signal Beam. J. Optical Society of America, vol. 59, January 1969, p. 10.

## REFERENCES (Concluded)

41. Fried, D. L. and Yura, H. T.: Telescope-Performance Reciprocity for Propagation in a Turbulent Medium. J. Optical Society of America, vol. 62, April 1972, p. 600.
42. Thomson, A. and Dorian, M. F.: Heterodyne Detection of Monochromatic Light Scattered from a Cloud of Moving Particles. General Dynamics/Convair, San Diego, California, CDC-ERR-AN-1090, June 1967.
43. Sonnenschein, C. H. and Horrigan, F. A.: Signal-to-Noise Relationships for Coaxial Systems that Heterodyne Backscatter from the Atmosphere. Applied Optics, vol. 10, July 1971, p. 1600.
44. Krause, M. C.; Morrison, L. K.; Craven, C. E.; Logan, N. A.; and Lawrence, T. R.: Development of Theory and Experiments to Improve Understanding of Laser Doppler Systems. Lockheed Missiles and Space Company, Huntsville, Alabama, LMSC-HREC TR D306632, June 1973.
45. Hufnagel, R. E. and Stanley, N. R.: Modulation Transfer Function Associated with Image Transmission Through Turbulent Media. J. Optical Society of America, vol. 54, January 1964, p. 52.
46. Pearson, Karl: Tables of the Incomplete  $\Gamma$ -Function, University Press, Cambridge, England, 1957.

## APPROVAL

### LASER DOPPLER SYSTEMS IN ATMOSPHERIC TURBULENCE

By S. S. R. Murty

The information in this report has been reviewed for security classification. The report, in its entirety, has been determined to be unclassified and contains no information concerning Department of Defense or Atomic Energy Commission programs.

This document has also been reviewed and approved for technical accuracy.

F. Brooks Moore

F. BROOKS MOORE

Director, Electronics and Control Laboratory